Proceedings of Medical Image Understanding and Analysis 99, Oxford: BMVA, 49-52.

A skin imaging method based on a colour formation model and its application to the diagnosis of pigmented skin lesions

Symon Cotton[1], Ela Claridge[2†] and Per Hall[3]

[1] Cambridge Design Partnership, Toft, Cambridge CB3 7RY.
[2] School of Computer Science, The University of Birmingham, Birmingham B15 2TT.
[3] Addenbrooke's Hospital, Cambridge CB2 2QQ.

Abstract. Pigmented lesions with different histology can appear similar, making clinical diagnosis of malignant melanoma difficult. This paper describes a new computer-based approach which uses an optical model of the skin to interpret the colours occurring in a lesion in terms of lesion histology. Through the development of an optical image formation model of human skin it is shown that all normal skin colours lie on a two-dimensional surface patch within a three-dimensional colour space. The colour coordinates corresponding to atypical skin structures deviate in characteristic ways from the predicted normal surface patch and thus can be identified. In particular, the method generates parametric images showing the presence of melanin in the dermis. This information can help in lesion discrimination.

1. Introduction

1.1 Pigmented skin lesions and malignant melanoma

Pigmented skin lesions occur where there is excessive melanin concentration in the skin. In benign lesions, melanin deposits are normally found in the epidermis and sometimes in the dermis. Apparent pigmentation can also occur as the result of the papillary dermis becoming thin. Sometimes small deposits of blood or concentration of small blood vessels can take the appearance similar to a pigmented skin lesion.

In malignant melanoma, melanocytes - the pigment forming cells of the skin - reproduce at the high, abnormal rate. Whilst they (and their associated melanin) remain in the epidermis, melanoma is termed "in situ" and, at this stage, it is not life-threatening. When they have penetrated into the dermis, the likelihood of metastases increases with the depth of penetration and patient prognosis becomes increasingly worse. It is crucial, therefore, that transformation to malignancy be detected at, or before the time the dermo-epidermal junction is breached.

The clinical diagnosis of melanoma is not always easy even for specialists, because malignant and benign lesions may look alike [1][2]. There is a widely acknowledged need amongst medical professionals for an aid to reliably distinguish melanoma from innocent pigmented lesions.

1.2 A new skin imaging method

We have recently developed a new method of interpretation of optical (digital) images of the skin, which allows us to derive histologically-related information from colour and near-infrared images. The hypothesis underlying our approach is that, since the external appearance of a skin lesion is formed by the interaction of light with the internal structure then it may be possible to infer the structure of the interior from the external appearance. The method proceeds in two stages. First, we construct an abstract model of colouration associated with the normal skin. The model is based on the physics governing interactions of light with the optical components of the skin. Image colours corresponding to the normal skin structure can be then interpreted via references to this model. In the second step, abnormal skin structures can be detected, because the skin colours associated with them do not conform to the normal skin colour model.

2. Optical model of the skin

Optically, the skin can be considered to be a layered structure of materials with different properties. In the upper layer, the epidermis, the main optical effect is absorption by pigment melanin, whereas in the dermis below the light is scattered through interaction with structural components of the skin and absorbed predominantly by haemoglobin in the blood.

2.1 Image formation model

Interaction of light with the skin structure is modelled using the Kubelka-Munk theory of scattering and absorption in inhomogeneous materials [3]. The radiation passing through an inhomogeneous translucent material is divided into two opposing diffuse fluxes: the radiant flux, I(d), in the direction of increasing sample depth d; and the flux J_0, returned to the

† Correspondence to: E.Claridge@cs.bham.ac.uk

surface as a result of scattering up to the depth d. The expressions R(d) and T(d) are the ratios relating I(d) and $J_0(d)$ to the incident radiation I_0:

$$R = \frac{J_0(d)}{I_0} \quad \text{and} \quad T = \frac{I(d)}{I_0} \tag{1}$$

To compute R and T for a given tissue, the inputs required are the depth d, the fraction of radiation absorbed per unit path length, α, and the fraction of radiation scattered per unit path length, ς [3] (α and ς are experimental constants, available from literature, e.g. [4]). To reflect the fact, that α and ς are wavelength (λ) dependent, R and T are denoted as $R(\lambda,d,\alpha,\varsigma)$ and $T(\lambda,d,\alpha,\varsigma)$.

Given the spectral composition of the incident light, $I_0(\lambda)$, the spectral composition of the light remitted from a tissue, $S_R(\lambda)$, and the light transmitted through the tissue, $S_T(\lambda)$, are:

$$S_R(\lambda) = R(\lambda,d,\alpha,\varsigma)\, I_0(\lambda) \tag{2}$$

$$S_T(\lambda) = T(\lambda,d,\alpha,\varsigma)\, I_0(\lambda) \tag{3}$$

Extending a two layer model described by (2) and (3) to an n layered system results in values for $R_{12...n}$ and $T_{12...n}$

$$R_{12...n} = R_{12...n-1} + \frac{T^2_{12...n-1} R_n}{1 - R_{12...n-1} R_n} \tag{4}$$

and

$$T_{12...n} = \frac{T_{12...n-1} T_n}{1 - R_{12...n-1} R_n} \tag{5}$$

This system of equations can compute the total remitted and transmitted light, $S_R(\lambda)$ and $S_T(\lambda)$, for an n layered system of arbitrary complexity, provided that the thickness and composition of the layers is specified. The resulting $S_R(\lambda)$ can then be used to predict the values of the chosen primaries, given their spectral characteristics. For example RGB primaries for the remitted light are computed as:

$$r = \int_0^\infty R(\lambda,d,\alpha,\varsigma)\, I_0(\lambda) S_r(\lambda) d\lambda, \qquad g = \int_0^\infty R(\lambda,d,\alpha,\varsigma)\, I_0(\lambda) S_g(\lambda) d\lambda, \qquad b = \int_0^\infty R(\lambda,d,\alpha,\varsigma)\, I_0(\lambda) S_b(\lambda) d\lambda \tag{6}$$

Thus, given a set of parameters characterising the skin structure and its optical composition [4], the model described above generates the skin colouration in terms of specified primaries. By systematically varying the physical parameters of the skin, we then investigated how changes in the skin structure and composition affect the distribution of colours in a colour space.

2.2 Optical model of the normal skin colouration

By spanning the range of coefficients for haemoglobin and melanin occurring in the normal skin, the model generated all possible skin colours. In particular, it predicted that the locus of all normal skin colours forms a simple surface patch within a three-dimensional colour space (Figure 1, left). The patch is bound by two physiologically-meaningful (and mathematically independent) axes corresponding to the amounts of the epidermal melanin and the dermal blood.

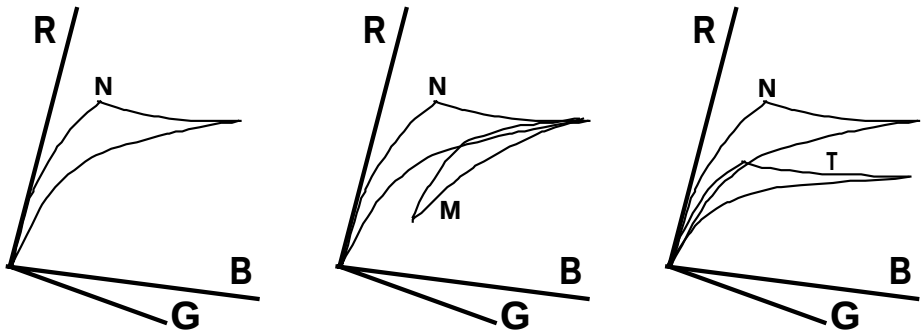

Figure 1. Left: the curved surface patch (N) shows the region of a 3-dimensional colour space (RGB) occupied by normal skin colours; Centre: normal skin colouration (N) together with the colouration associated with melanin descent (M); Right: normal skin colouration (N) together with the colouration associated with thinned papillary dermis (T).

These predictions have been successfully verified by comparing the theoretical colour distribution with colour distribution derived from cross-racial sample of over fifty skin images [5]. The comparisons made in the LMS colour space showed that for the L primary 86% of measured LMS values lie within a single standard deviation of the model, with 78% and 82% for the M and S primaries respectively. In view of this, the model can be considered valid within the bounds of experimental errors [6].

2.3 Modelling abnormal skin architectures

As the next step we modelled architectural changes within the skin. In the first instance we considered the descent of melanin into the dermis, which occurs in invasive melanoma. This condition makes the skin colours depart from their normal location in the colour space along characteristic paths specified by the depth of melanin descent and by melanin concentration (Figure 1, centre). Thus, theoretically, any colours present in a skin image which deviate in the same way from the normal location in the colour space, should indicate the presence of melanin in the dermis and therefore be of diagnostic value. Further analysis of the effects of different model parameters on the resulting colours revealed, however, that the colours resulting from a decrease in thickness of the papillary dermal layer (whose thickness p_0 in the normal skin is assumed to be 0.2mm) may occupy the same position in the colour space as colours due to melanin descent (Figure 1, right). This may explain the difficulties in differentiating on the basis of colour alone between melanoma and certain other skin lesions in which this condition occurs [7][8].

We were able to estimate the thickness of the papillary dermis by the analysis of images obtained in two near-infrared (NIR) bands. In this part of the spectrum the absorption by melanin and blood become relatively small [9] and the papillary dermis is the main optically responsive component. The difference in the amount of light backscattered at two different NIR bands allows us to estimate the papillary dermis thickness, p. With this quantity known, the colour coordinates of all the image points at p are then adjusted to the corresponding coordinates at thickness p_0 assumed by the normal skin model. Any colours, which after this adjustment still do not lie on the surface of normal skin colouration, are deemed to be caused by the presence of melanin in the dermis.

3. Model based image interpretation

The analysis of the image formation process as described above has resulted in a model of skin colouration for both normal and abnormal conditions. This model enables interpretation of colours in images of the skin in terms of parameters which can be related to skin anatomy and physiology. Given one colour (RGB) and two infrared images, all calibrated, the following parameters can be derived *for each point within the image*: amount of epidermal melanin; amount of blood within the dermis; thickness of the papillary dermis and the presence of dermal melanin. These quantities are represented as *parametric images* which can be either viewed by a clinician or subjected to further image analysis. Information contained in these images is complementary to that which can be obtained through normal visual examination and thus it is likely to help in differential diagnosis.

The first step of the process is to estimate the thickness of the papillary dermis from a pair of infra-red images. This will generate a parametric image showing the thickness of the papillary dermis at each point of the skin. If the thickness differs from that assumed by the model, the colour of a given point is adjusted to correspond to the “standard” thickness. Next, the amount of dermal blood is obtained by de-referencing a given colour location on the surface of normal skin colouration [5][10] and a corresponding parametric image is created. If the melanin is present in the dermis, its presence can be detected from the fact, that even after the papillary dermis thickness adjustment which may have been carried out in the first step, the colours still do not lie on the surface of normal skin colouration. A parametric image created through this part of analysis, shows the locations where melanin is present in the dermis. Finally, the amount of epidermal melanin is obtained (at present only for the skin locations which do not contain melanin in the dermis), again by de-referencing skin colour locations on the surface of normal skin colouration. For other locations this amount can only be estimated. The model analysis showed that the amount of melanin and the depth of melanin penetration into the dermis can only be reliably estimated up to 0.06mm. Beyond that, the decrease in the amount of back-scattering collagen, combined with the increase in the light-absorbing melanin, cause the amount of remitted light to decrease below the noise level of the imaging system.

4. Results

The method was first tested on computer-generated phantoms of the skin and it was shown to be feasible [5][10]. In view of the positive results, the method was applied to real skin images obtained from the Addenbrooke’s Hospital Plastic Surgery Department. To date we have clinically verified only measurements related to one of the parameters, the presence of melanin in the dermis. This is diagnostically the most important parameter. Moreover, the verification was possible because the routine biopsy examinations always return this result. Verification of other parameters is more difficult as they are not a subject of routine laboratory tests.

In the pilot study we have analysed six lesions with confirmed histological diagnoses, three containing melanin in the dermis and thus warranting the excision (two lentigo maligna lesions - without melanin in the dermis, two superficial spreading melanomas - one with dermal invasion, and two compound naevi - both containing melanin in the dermis) [9]. The objective was to establish, through the model-based analysis applied blindly to the lesion images, whether the lesions contain melanin in the dermis. In all the six cases the results of computer analysis were in agreement with histological diagnosis; interestingly, three lesions from this set were mis-diagnosed by clinical (i.e. visual) examination. Figure 2 illustrates one set of the results.

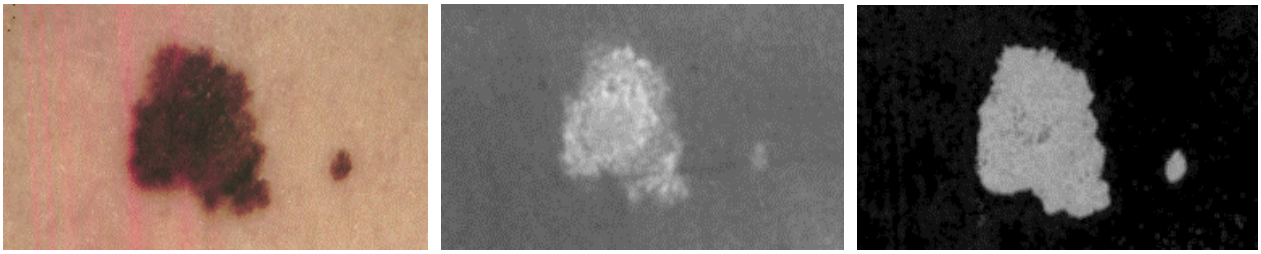

(a) (b) (c)

Figure 2: (a) Compound naevus (original image); (b) A parametric image showing thickness of the papillary dermis (thickness is proportional to image brightness); (c) A parametric image with bright areas showing the presence of melanin in the dermis.

5. Discussion and conclusions

The results reported in this paper, although practically applied only to a very small number of real images, appear very promising. The theoretical analysis showed that the method is very sensitive at detecting the presence of melanin just below the dermo-epidermal junction, at a penetration depth into the dermis as small as 0.05 mm. It is thus an ideal tool for detecting melanin invasion before it becomes life-threatening.

The clinical verification and evaluation of utility of other parameters that our method can compute (the amount of epidermal melanin, the amount of dermal blood, thickness of papillary dermis layer and, in the presence of melanin descent, the position and concentration of melanin within the dermis) is planned for the near future. To date, for some of the features there are no established in vivo measurement, grading or detection methods. Consequently, little is known about their predictive value in detecting early signs of melanoma. The increased blood supply in vicinity of the lesion, the thickening of the papillary dermis as the side-effect of the body defence mechanism, and the irregular depth of dermal melanin, have all been suggested as having a potential association with melanoma.

In the long term, a device could be made available to GPs, who are the first point of referral in UK; assistance in diagnosis of melanoma could thus be offered on a really broad basis.

References

1. Mihm M (1997) Benign lesions that simulate malignant melanoma. *Melanoma Research* **7**, 48-49.
2. Barnhill R (1997) Malignant lesions that look benign. *Melanoma Research* **7**, 49.
3. Egan WG, Hilgeman TW (1979) *Optical Properties of Inhomogeneous Materials*: Academic Press.
4. Anderson R, Parrish BS, Parrish J (1981) The optics of human skin. The Journal of Investigative Dermatology 77(1), 13-19.
5. Cotton SD, Claridge E (1996) Developing a predictive model of human skin colouring, Vanmetter RL, Beutel J (Eds.) *Proceedings of the SPIE Medical Imaging 1996* vol. 2708, 814-825.
6. Lyons L (1991) *A Practical Guide to Data Analysis for Physical Science Students*: Cambridge
7. Perednia D, Gaines J, Rossum A (1992) Variability in physician assessment of lesions in cutaneous images and its implications for skin screening and computer-assisted diagnosis. *Archives of Dermatology* **128**, 357-364.
8. Durg A, Stoecker W, Cookson J, Umbaugh S, Moss R (1993) Identification of variegated coloring in skin tumors - Neural Network vs Rule-based induction methods. *IEEE Engineering in Medicine and Biology Magazine* **12**, 71.
9. Cotton SD (1998) *A non-invasive imaging system for assisting in the diagnosis of malignant melanoma*. PhD Thesis, The University of Birmingham.
10. Cotton SD, Claridge E, Hall PN (1997) Noninvasive skin imaging, *Information Processing in Medical Imaging* (Springer-Verlag, LNCS 1230), 501-507.